THE INFLUENCE OF CLEARANCES IN A DRIVE SYSTEM ON DYNAMICS AND KINEMATICS OF A TELESCOPIC CRANE

Arkadiusz TRĄBKA*

*Faculty of Mechanical Engineering and Computer Science, Department of Engineering Fundamentals, University of Bielsko-Biala, ul. Willowa 2, 43-309 Bielsko-Biała, Poland

atrabka@ath.bielsko.pl

Abstract: The paper presents the results of numerical analyses that were carried out in order to evaluate how a change in a size of a clearance in a slewing motion drive system of a telescopic crane influences the movement of a load and the dynamic loads of a structure. A computational model was developed based on a real structure of an experimental crane by using the ADAMS software. The analyses showed that a circumferential clearance at the output of a reduction gear, which is less than 1º, does not adversely affect the precision of the load movement. An excessive clearance leads to losing fluidity of a body slewing motion and to changes in the trajectory of the load.

Key words: Clearances, Drive System, Experimental Telescopic Crane, Multibody Dynamic Systems

1. INTRODUCTION

Kinematic and dynamic analysis of systems with a complex kinematic structure is mostly done based on numerical models. Many phenomena that occur in real structures are usually neglected in these models. Clearance in joints of structural components is one of the most frequently neglected phenomenon. Omission of clearances simplifies analysis, but at the same time makes that the results may significantly differ from reality. Confirmation of this can be found in various works. Authors of this works have studied the influence of the clearance in kinematic pairs on the kinematic and/or dynamic properties of various kinds of mechanisms, e.g. a slider-crank (Flores, 2010; Flores and Ambrosio, 2004; Flores et al., 2010; Olivier and Jesus, 2002), a yoke (Olivier and Jesus, 2002), a four-bar linkage (Bai and Zhao, 2012; Tian et al., 2009; Ting et al., 2000), a parallel manipulator (Parenti-Castelli and Venanzi, 2005; Ting et al., 2000), an open manipulator with two link arms (Zhao and Bai, 2011), an open manipulator with four link arms (Harlecki, 1999) and an industrial robot manipulator (Erkaya, 2012; Pan et al., 1998).

Taking into account clearances in drive systems is very important for the proper mapping of real systems. Clearances in these systems may occur in various types of joints, for example parallel key, splined and coupling. However, due to design a sumptions the clearances are mainly present at the interface of gear wheels in toothed gears (Oberg et al., 2004). The influence of the clearance between the teeth of wheels on the dynamic properties of different types of gears (planetary, single-stage and two-stage) has been shown in Kuusisto (1999); Siyu et al., (2011); Sun and Hu (2003); Walha et al. (2009).

Cranes with telescopic booms are examples of real systems with complex kinematic structure (Trąbka, 2014a). Their computational models usually are considered as devoid of clearances, whereas they occur both in joints of structural components and in drive systems. Clearances in computational models of cranes were encountered only in two works among the reviewed papers. In Harlecki (1998) the clearance was taken into account in joints between supporting beams and guides of a crane frame, while in Trombski et al. (1995) the clearance between members of a telescopic boom was considered. None of the reviewed papers contains a model taking into account clearances in a crane drive system.

The drive systems are one of the most important systems of telescopic cranes that determine the precision of a load motion. Their structure should provide the possibility to execute the load motion in accordance with the planned trajectory. This trajectory can significantly change due to presence of excessive clearances between components of the drive system.

This paper presents the results of numerical analyses of a computational model of an experimental telescopic crane that were carried out in order to evaluate how a change in a size of a circumferential clearance, at the output of a reduction gear of a slewing motion drive, influences the movement of a load and the dynamic loads of a structure.

2. COMPUTATIONAL MODEL OF A CRANE

The crane model was developed in two stages. First, the Inventor program was used to build a geometric model. This model was developed based on the real structure of an experimental crane (Fig. 1a). In the second stage, the computational model was developed (Fig. 1b). It was made by using the ADAMS multibody system analysis software.

The computational model included the majority of the experimental crane structural components. Only some fasteners and wires of little significance for the dynamics of the structure were omitted. A reduction gear of the body slew drive was made as the system of three elements, i.e. a gear joint, a coupling with adjustable size of a circumferential clearance and a torsion spring with a vibration damper (see detail in Fig. 1b). Joints between structural components were selected to map accurately the real object

DOI 10.1515/ama-2015-0002

movement possibilities. Particular attention was paid to prevent the occurrence of so-called redundant constraints. The dimensions, masses and mass moments of inertia of the model parts were determined based on measurements of the real structure and the geometrical models of these parts, which had been developed by using the Inventor software (Tab. 1).

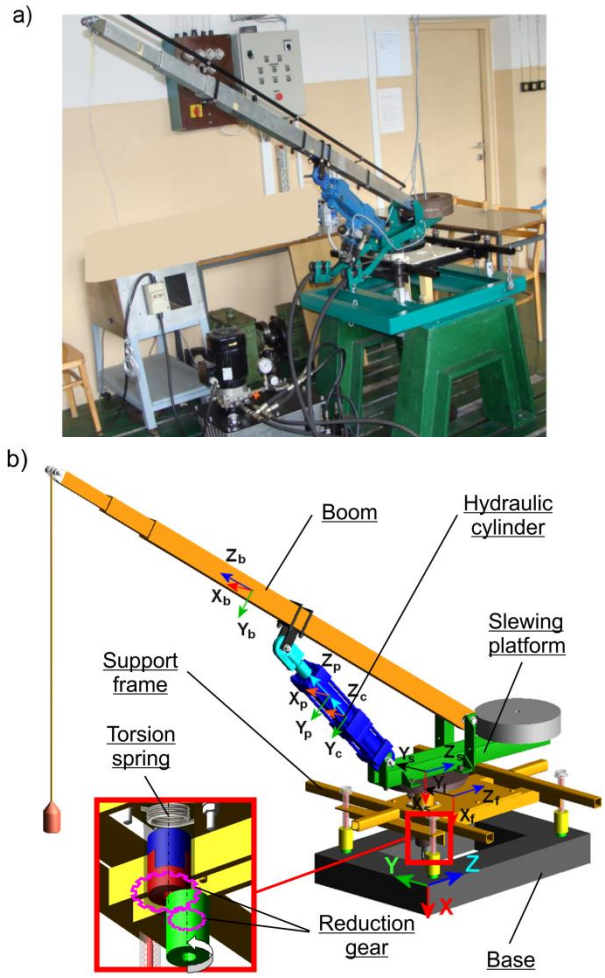

Fig. 1. a) Experimental telescopic crane (Trąbka, 2014b), b) Computational model

The possibility of deformations was taken into account in the model only in supports and in the body slew drive. A support system with the supports having bilateral constraints was used (Trąbka, 2014b). The stiffnesses of vertical springs that were used to model the supports (Fig. 2) were determined experimentally. The same stiffness was adopted for all springs. This stiffness was determined for a spring that was randomly selected from the set of springs based on a series of 10 measurements of the dependence of deformation on the load. For each dependence of deformation on the load, an average stiffness k_N was calculated based on equation (1) and then a substitute stiffness $k_x = 17.25 \times 10^3 \mathrm{N/m}$ was determined by using equation (2). Apart from axial stiffnesses also the stiffnesses of pairs of springs, perpendicular to their axes, were taken into account. Lateral stiffnesses of the pairs of springs ($k_y = k_z = 114 \times 10^3 \mathrm{N/m}$) were determined numerically. Both the computational model and the calculations were made using the Ansys v11 software and following a method described in Kłosiński and Trąbka (2010).

$$k_N = \frac{1}{m} \cdot \sum_{i=1}^{i=m} \frac{\Delta P_i}{\Delta l_i} \tag{1}$$

$$k_x = \frac{1}{s} \cdot \frac{1}{n} \cdot \sum_{N=1}^{N=n} k_N \tag{2}$$

where: N – measurement number, m – number of changes in a spring load, s = 2 – number of springs that are connected in parallel to each other in a crane support model, n – number of measurements, ΔP_i – i-th change in the load carried by a spring, Δl_i – i-th change in a spring length.

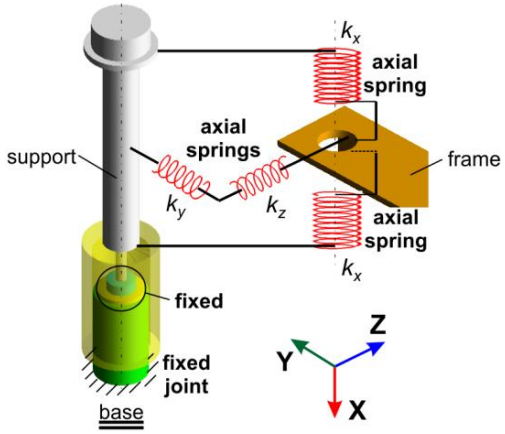

Fig. 2. Support model (Trąbka, 2014b)

Tab. 1. Masses and mass moments of inertia of the model parts

Name of a given part	Mass [kg]	Mass moments of inertia with respect to the centres of masses of the model parts [kg·m²]		
		J_{sx}	J_{sy}	J_{sz}
Support frame	17.3	0.792	0.567	0.235
Slewing platform	20.2	0.688	0.706	0.128
Counterweight	17	0.175	0.094	0.094
Boom	4.5	0.937	0.936	0.0025
Piston rod	3.7	0.068	0.067	0.0008
Cylinder	11	0.21	0.21	0.01
Reductor	10.5	0.003	0.003	0.0002

Damping coefficients c_u in the supports (systems of springs) were calculated, by using equation (3), for the directions of the X, Y and Z-axes of a reference frame. These calculations were based on the changes in position of the support frame with respect to the base (Giergiel, 1986).

$$c_u = \frac{2 \cdot M \cdot \delta}{T} \tag{3}$$

where: M – mass connected with the system of supports (which depends on the location of the sensor of displacements and the direction of movement), δ – average value of the logarithmic damping decrement (based on equation (4)), T – average value of a period of the damped vibration (based on equation (5)).

$$\delta = \frac{1}{2} \cdot \left[\ln\left(\frac{1}{k} \cdot \sum_{i=1}^{i=k} \frac{A_i}{A_{i+1}} \right) + \ln\left(\frac{1}{l} \cdot \sum_{j=1}^{j=l} \frac{A_j}{A_{j+1}} \right) \right] \tag{4}$$

where: k – number of amplitudes in the upper part of the characteristics (included in the calculations), l – number of amplitudes in the bottom part of the characteristics (included in the calculations),

A_i, A_j – amplitudes for the upper and the lower part of the characteristics, A_{i+1}, A_{j+1} – subsequent amplitudes for the upper and the lower part of the characteristics.

$$T = \frac{1}{2} \cdot \left[\frac{1}{p} \cdot \sum_{i=1}^{i=p} T_i + \frac{1}{r} \cdot \sum_{j=1}^{j=r} T_j \right] \quad (5)$$

where: p – number of periods in the upper part of the characteristics (included in the calculations), r – number of periods in the bottom part of the characteristics (included in the calculations), T_i – partial periods in the upper part of the characteristics, T_j – partial periods in the bottom part of the characteristics.

For every direction of movement, 10 measurements were carried out and the average damping coefficients c_s were calculated based on these measurements. Finally, the following values were adopted for calculations: $c_{sx} = 0.28 \times 10^3 \mathrm{N} \cdot \mathrm{s/m}$, $c_{sy} = 0.47 \times 10^3 \mathrm{N} \cdot \mathrm{s/m}$, $c_{sz} = 0.59 \times 10^3 \mathrm{N} \cdot \mathrm{s/m}$.

The stiffness of the body slew drive ($k_{\alpha r} = 7.386 \times 10^3 \mathrm{N} \cdot \mathrm{m/rad}$) was determined based on a separate model (Fig. 3). This model was developed in the ADAMS program based on the structure of the Befared 7-AP-RM-2-V6 two-stage reduction gear (with a gear ratio $i = 20$), which was used to drive the experimental crane. Deformations of shafts, parallel key connections and gears were included in the above model using torsion springs. These springs were inserted between rigid solid elements. Torsional stiffnesses were calculated for the particular components based on the formulas shown in Table 4.1 in Marchelek (1991).

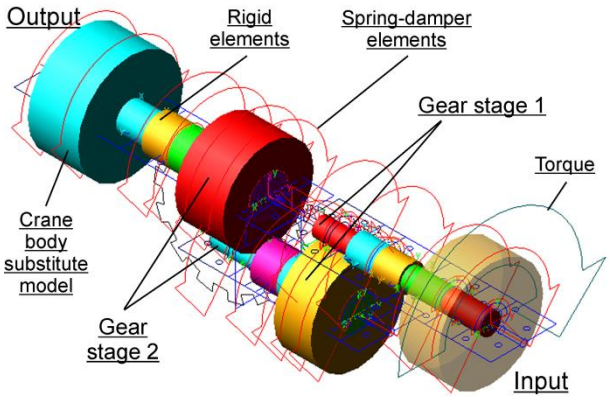

Fig. 3. Model of the body slew drive

The model shown in Fig. 3 was also used to determine a substitute damping coefficient of the slew drive ($c_{\alpha r} = 9.16 \mathrm{N} \cdot \mathrm{m} \cdot \mathrm{s/rad}$). Based on equation (6) the damping coefficients $c_{\alpha i}$ of the power transmission components were determined (Marchelek, 1991):

$$c_{\alpha i} = k_i \cdot T_i \quad (6)$$

where: k_i – stiffness coefficient of i-th component, T_i – time constant of i-th component (taken from Table 4.4 in Marchelek (1991)).

The calculated coefficients were assigned to the individual torsion springs and then the analysis of damped free vibrations of the substitution model of the body was performed (the substitution model parameters were obtained by the reduction of the body mass as well as its mass moments of inertia to the drive output).

The substitute damping coefficient of the slew drive was calculated from equation (7) (Żółtowski, 2002).

$$c_{\alpha r} = \frac{\delta}{\pi} \cdot \sqrt{J_z \cdot k_{\alpha r}} \quad (7)$$

where: δ – average value of the logarithmic damping decrement (based on equation (4)), J_z – mass moment of inertia of the body substitution model, calculated with respect to its axis of rotation, $k_{\alpha r}$ – stiffness of the slew drive of the body.

Spring-damper properties of the drive were introduced into the model as the parameters of the torsion spring. This spring was inserted between the coupling (modelling a clearance zone at the output of the reduction gear) and the axis of rotation of a slewing platform (see the torsion spring in Fig. 1b).

3. RESULTS AND DISCUSSION

This paper presents an evaluation of the influence of the clearance size, in the slewing motion drive system of the telescopic crane body, on the load trajectory, the speed of rotation of the body and the support loads.

The calculations were carried out for a crane radius of 1.43 m, a rope length of 1 m and a load mass of 1 kg. It was assumed that the initial position of the computational model corresponds to a crane being in a state of static equilibrium; the initial tension of springs, used to model the supports, was taken into account (their values were taken as consistent with registered during the tests of the experimental crane). The rotation of the body relative to a chassis by an angle of 90º was analysed. The kinematic input function (Fig. 4) and a constant step of integration (Δt = 0.001 s) were used.

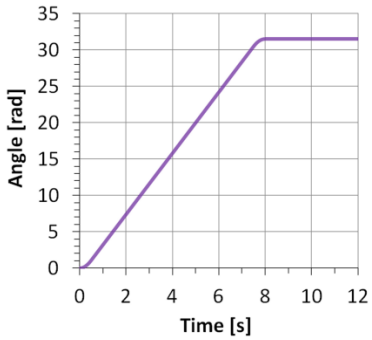

Fig. 4. Slewing motion input function

The model without circumferential clearance at the reduction gear output as well as with clearances of the values 0.5º, 1.0º, 1.5º, 2.0º, 2.5º, 3.0º, 3.5º, 4.0º, 4.5º and 5.0º was analysed. The clearance was introduced both on an active side (designation CA) as well as on a passive side (designation CB); wherein on the passive side its value was always 0.5° (Fig. 5).

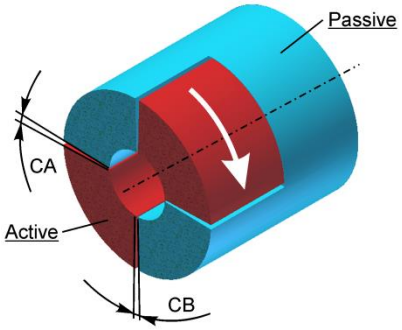

Fig. 5. Clearance model

DOI 10.1515/ama-2015-0002

The computational model was verified experimentally. This verification was conducted by comparing the calculated support loads with the loads that were recorded during the tests of the experimental crane with 3º clearance at the output of the reduction gear. The comparison result is shown in Fig. 6a. It was found that the model properly map the real object, and the visible differences between characteristics are due to the omission of the flexibilities of particular parts (especially the boom), the flexibilities of joints, the friction in joints, and most of all due to the omission of clearances at the supports.

The calculation results for the model without clearance and with clearances of 1.0º, 3.0º and 5.0º are presented in Figs. 6b-d. Fig. 6b presents the trajectory of the mass centre of the load while Fig. 6c shows the changes in the speed of rotation of the body relative to the chassis. The distribution of the support loads is shown in Fig. 6d.

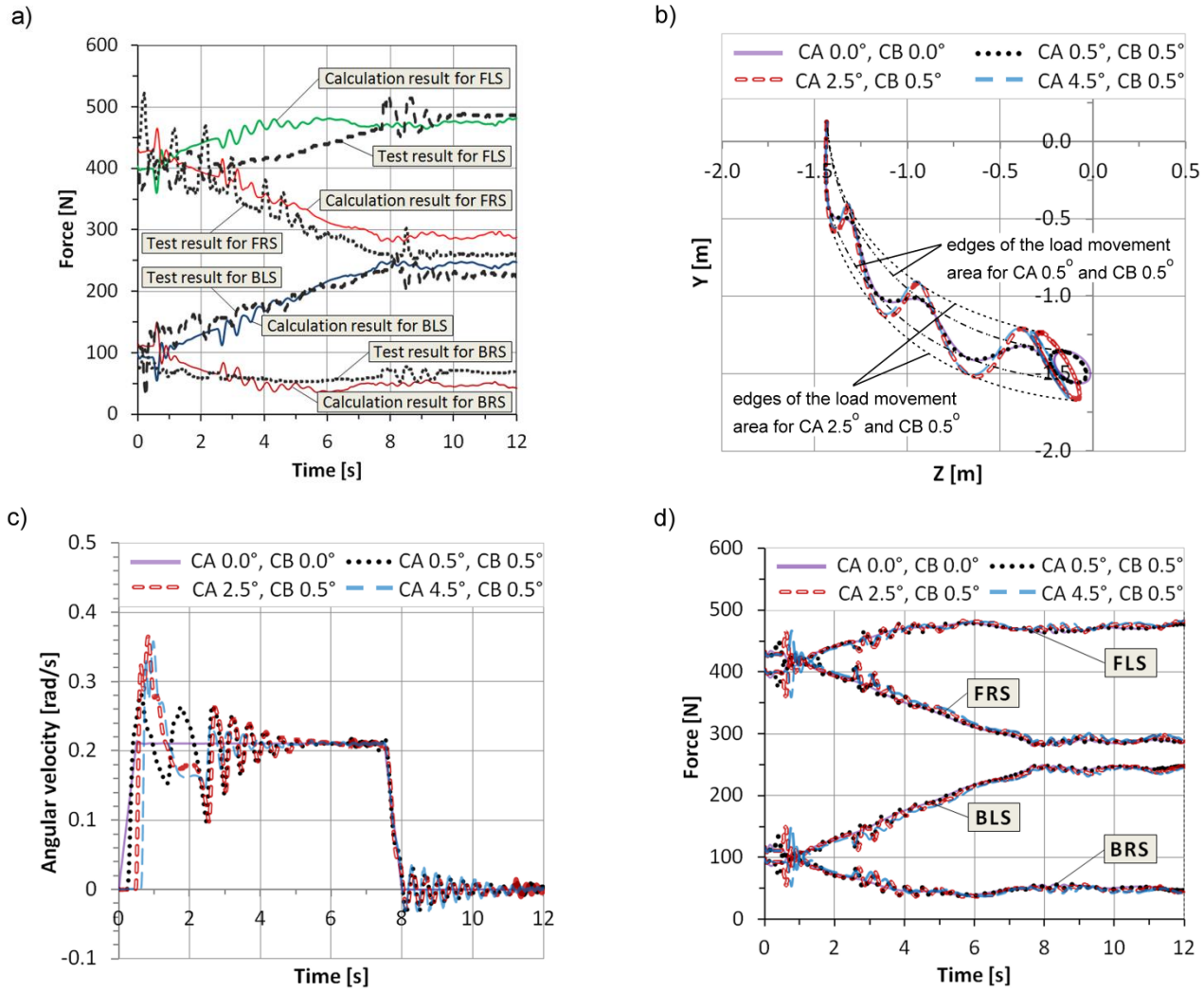

Fig. 6. Calculation results: a) comparison of the support loads - calculated with the one that were recorded during the tests (for 3º clearance), b) trajectory of the mass centre of the load, c) speed of rotation of the body relative to the chassis, d) distribution of the support loads (FLS – front left support, FRS – front right support, BLS – back left support, BRS – back right support)

Based on the calculation results (Figs. 6b-d) it was found that:

- The trajectory of the load is not subject to significant changes if the circumferential clearance at the output of the reduction gear does not exceed 1º. When the clearance increases in the range of 1º to 3º the load swings are increasing in the direction of radial and tangential components. As a result, the trajectory of the load is changing both during the rotation and after stopping of them. Further increase of the clearance (in the range of 3º to 5º) contributes to a slight reduction in the load swings.
- The load swings after stopping of the slewing motion, due to an excessive clearance at the output of the reduction gear, can be up to 73.7% higher than in the model without the clearance (for the clearance equal 4º).
- Even a small clearance at the output of the reduction gear causes that the speed of rotation of the body undergoes constant changes. The changes in the speed of rotation are closely related to the vibrations of the body whose amplitude and frequency depends on the size of the clearance, the stiffness and the damping in the drive system. The largest change of the speed in relation to the value obtained for the model without clearance was 73% when the clearance was 3º.
- The maximum changes in the load of supports occur during the start-up. They are greater the larger is the clearance, and at the same time, the higher value achieves acceleration when

the clearance is deleted. The largest change of the load in relation to the value obtained for the model without clearance was 53% when the clearance was 4º.

4. CONCLUSIONS

This paper presents the results of numerical analyses of a computational model of an experimental crane that were carried out in order to evaluate how a change in a size of a circumferential clearance, at the output of a reduction gear of a slewing motion drive, influences the movement of a load and the dynamic loads of a structure. Based on the numerical analyses, it has been found that:

- The circumferential clearance, which is less than 1º, does not adversely affect the precision of a load movement. The maximum excess of the support loads for 1º amount of the clearance does not exceed 14.7% of the value obtained for the model without the clearance.
- When the clearance increases in the range of 1º to 3º both the load swings and the vibration amplitudes of a body are increasing too. As a result, the area in which a load moves becomes wider (Fig. 6b). Pulsed changes in the load of supports increase, wherein the largest values of the dynamic excess with respect to the value determined for the model without clearance (ΔQ = 43.5% for the clearance equal 3º) are obtained during the start-up. They are greater the higher value achieves acceleration during the start-up.
- Increasing of the clearance in the range of 3º to 5º means a further (but much less than in the range of 1º to 3º) increase of the dynamic excess of the support loads. However, the load swings are slightly smaller, especially those that occur after stopping the slewing motion.

The above observations show that clearances should be controlled in drive systems of telescopic cranes, as even slight increasing of them above values established by the designers leads to a significant worsening of their kinematic and dynamic properties.

REFERENCES

1. **Bai Z.F., Zhao Y.** (2012), Dynamics modeling and quantitative analysis of multibody systems including revolute clearance joint, *Precision Engineering*, 36, 554– 567.
2. **Erkaya S.** (2012), Investigation of joint clearance effects on welding robot manipulators, *Robotics and Computer-Integrated Manufacturing*, 28, 449–457.
3. **Flores P.** (2010), A parametric study on the dynamic response of planar multibody systems with multiple clearance joint, *Nonlinear Dynamics*, 61, 633–653.
4. **Flores P., Ambrosio J.** (2004), Revolute joints with clearance in multibody systems, *Computers and Structures*, 82, 1359–1369.
5. **Flores P., Leine R., Glocker R.** (2010), Modeling and analysis of rigid multi-body systems with translational clearance joints based on the nonsmooth dynamics approach, *Multibody System Dynamics*, 23 (2), 165–190.
6. **Giergiel J.** (1986), *Damping of mechanical vibrations* (in Polish), Wyd. AGH, Kraków.
7. **Harlecki A.** (1998), Dynamic analysis of telescopic truck crane using the rigid finite element method, *Zeszyty Naukowe Politechniki Łódzkiej Filii w Bielsku-Białej, Budowa i Eksploatacja Maszyn*, 32 (51), 11-39.
8. **Harlecki A.** (1999), „Stick-Slip" motion of open manipulators with flexible drives and dry friction in joint, *Journal of Theoretical and Applied Mechanics*, 4 (37), 873-892.
9. **Kłosiński J., Trąbka A.** (2010), Frequency analysis of vibratory device model (in Polish). *Pneumatyka*, 1, 46-49.
10. **Kuusisto S.** (1999), Transient nonlinear dynamics of camshafts, *Proceedings of the IMAC 17th international modal analysis conference*, 1093-1099.
11. **Marchelek K.** (1991), *Machine tools dynamics* (in Polish), WNT, Warszawa.
12. **Oberg E., Jones F.D., Horton H.L., Ryffel H.H.** (2004), *27th Edition Machinery's Handbook*, Industrial Press, Inc., New York.
13. **Olivier B.B.A., Jesus R.** (2002), Modeling of joints with clearance in flexible multi-body system, *International Journal of Solids and Structures*, 39, 41–63.
14. **Pan M., Van Brussel H., Sas P.** (1998), Intelligent joint fault diagnosis of industrial robots, *Mechanical Systems and Signal Processing*, 12 (4), 571-588.
15. **Parenti-Castelli V., Venanzi S.** (2005), Clearance influence analysis on mechanisms, *Mechanism and Machine Theory*, 40, 1316–1329.
16. **Siyu C., Jinyuan T., Caiwang L., Qibo W.** (2011), Nonlinear dynamic characteristics of geared rotor bearing systems with dynamic backlash and friction, *Mechanism and Machine Theory*, 46, 466–478.
17. **Sun T., Hu H.Y.** (2003), Nonlinear dynamics of a planetary gear system with multiple clearances, *Mechanism and Machine Theory*, 38, 1371–1390.
18. **Tian Q., Zhang Y., Chen L., Flores P.** (2009), Dynamics of spatial flexible multibody systems with clearance and lubricated spherical joint, *Computers and Structures*, 87 (13-14), 913–929.
19. **Ting K.L., Zhu J., Watkins D.** (2000), The effects of joint clearance on position and orientation deviation of linkages and manipulators, *Mechanism and Machine Theory*, 35, 391-401.
20. **Trąbka A.** (2014a), Dynamics of telescopic cranes with flexible structural components, *International Journal of Mechanical Sciences*, 88, 162–174.
21. **Trąbka A.** (2014b), The impact of the support system's kinematic structure on selected kinematic and dynamic quantities of an experimental crane, Acta Mechanica et Automatica, vol.8, no.4, 189-193.
22. **Trombski M., Kłosiński J., Majewski L., Suwaj S.** (1995), Dynamic analysis of a crane model when the clearances in kinematic pairs of the crane jib are taken into account (in Polish), *Materiały VIII Konferencji „Problemy Rozwoju Maszyn Roboczych", Część I*, Zakopane, 191-198.
23. **Walha L., Fakhfakh T., Haddar M.** (2009), Nonlinear dynamics of a two-stage gear system with mesh stiffness fluctuation, bearing flexibility and backlash, *Mechanism and Machine Theory*, 44, 1058–1069.
24. **Zhao Y., Bai Z.F.** (2011), Dynamics analysis of space robot manipulator with joint clearance, *Acta Astronautica*, 68, 1147–1155.
25. **Żółtowski B.** (2002), *Research of machine dynamics* (in Polish), Wyd. MARKAR, Bydgoszcz.